

FROM MDO TO MANUFACTURING: APPLICATION CASE FOR UNMANNED AERIAL VEHICLES

Luiz F. T. Fernandez^{1,2*}, Murat Bronz², Thierry Lefebvre¹ and Nathalie Bartoli¹

1: ONERA/DTIS,
Université de Toulouse,
31400 Toulouse, France
{luiz.tiberio,thierry.lefebvre,nathalie.bartoli}@onera.fr

2: ENAC,
Université de Toulouse,
31400 Toulouse, France
murat.bronz@enac.fr

Abstract. *This paper explores the concept of coupling an MDO problem directly to a manufacturing process. The design parameters required for various disciplinary analyses are used to automatically generate geometries that comply with the selected manufacturing processes. Such geometries are then manufactured to validate our proposal. This strategy reduces the manufacturing time of unmanned aerial vehicles (UAVs) as the CAD modeling becomes automatic and parametric, also allowing for easier comparison of different geometries. It can also potentially improve the MDO process by closing the information loop with manufacturing constraints. We employ the Engineering Sketch Pad (ESP) and leverage from additive manufacturing techniques usually applied in UAVs. The choice of ESP facilitates reproducibility, as it is an operating system agnostic open source CAD, and gradient based optimization, due to its capability of computing gradients of the geometric outputs with respect to the design parameters. The manufacturing processes of wings and propellers are addressed. For the same representative wing geometry, we present different modeling strategies for mass and inertia prediction and for manufacturing using 3D printing. ESP is also employed to predict wing mass and inertia. The maximum difference in weight between the manufactured wing and its predicted value using ESP is roughly 7%. The propeller is 3D printed in resin with stereolithography (SLA) technique, and is defined by means of its airfoils, radius, and chord and twist angle distributions. We conclude about the applicability of the presented strategy, as well as its potential and limitations. All the scripts are shared with the community so researchers can apply it to validate their own MDO problem.*

Keywords: Additive Manufacturing, MDO of UAVs, UAV design and manufacturing

1 INTRODUCTION

With the establishment of unmanned aerial vehicles (UAVs), a significant increase in the interest in such kind of vehicle has been observed in recent years for several applications. Ranging from widespread ideas such as delivery of goods or search and rescue to more specialized ones, such as fire fighting [1–3], debris mapping [4], covid mitigation [5], and even nutrition delivery in the form of edible vehicles [6]. Within different configurations of UAVs, winged designs stand out when higher flight range and endurance are needed. Several manufacturing techniques have been applied for winged UAVs fabrication. In terms of wing manufacturing, hobbyists predominantly utilize balsa wood, which was primarily employed during the early stages of the UAV era. This conventional approach has subsequently been enhanced by combining balsa with composite materials, as in Chung *et al.* [7], and even full composite wings as in Nugroho *et al.* [8]. Full composite wings tend to be light and of high quality, but the manufacturing process is complicated and time consuming. Recently, there has been attention towards additive manufacturing techniques due to their ability to save time and material, fabricate complex geometries, and achieve higher levels of automation. Such techniques have been successfully applied in several cases. Bronz *et al.* [9] presented a 3D printing strategy for UAVs using Onyx material, a blend of carbon fiber and nylon, which provided the desired structural properties and surface quality while keeping a reasonable weight. Taylor *et al.* [10] and Muir *et al.* [11] coupled optimization processes to additive manufacturing techniques in order to obtain an aircraft structure and a mission optimized UAV, respectively. Laliberté *et al.* [12] used 3D printing to build a biologically inspired micro aerial vehicle. In 2015, Aurora Flight Sciences also presented the first jet-powered 3D-printed UAV [13]. While several other applications of additive manufacturing for UAVs can be found in the survey by Goh *et al.* [14], this technique has also been successfully employed for teaching activities [15] and even in experiments in hypersonic conditions [16]. For propellers, there are several off-the-shelf options commercially available. Their good quality combined with small prices is usually enough for the UAV community, which has not yet explored propeller design and manufacturing with the exception of a few studies, as in Rutkay and Laliberté [17]. We already employed additive manufacturing for propellers in [18], where a specific geometry was needed in order to compare different aerodynamic methodologies. The higher level of automation from 3D printing also facilitates the integration between design and fabrication processes. Such integration might be beneficial in two ways: enriching design and optimization process with manufacturing constraints, anticipating possible problems or even unfeasible designs; and reducing the time needed to complete the full cycle between design and flight. Regarding the insertion of manufacturing information within a multidisciplinary design and optimization (MDO) process, Laan *et al.* [19] used model-based system engineering techniques to account for the manufacturing cost of high lift devices in the design of experiments performed for the initial sizing of an aircraft. Doneli *et al.* [20, 21] also addressed, within the MDO, the choice of raw materials, manufacturing and assembly processes as well as the supply chain, ensuring a more realistic and comprehensive optimization process. In this paper, our focus is to present a viable way to automatically connect the output of a given MDO process to the fabrication of a UAV. The optimization loop is represented by means of its output design parameters or geometry, and the fabrication is performed with 3D printing. We leverage from the size and affordable characteristics of UAVs to fully test our proposal, presenting the entire

Table 1: Optimal design from [22]

Design variables	Value
Root chord	0.12 <i>m</i>
Tip chord	0.095 <i>m</i>
Wing span	0.7 <i>m</i>
Cruise α	10°
Turn α	8°
Battery mass	0.2 <i>kg</i>



Figure 1: 3D model and real vehicle from [22]

process, from modeling to real manufacturing, for wings and propellers. This paper is organized as follows: in Section 2 we present the context in which this study takes place. Section 3 explains how we share the data. The methodology and results are presented in Sections 4 and 5, respectively. Our conclusions and perspectives are then presented in Section 6.

2 CONTEXT

This paper is part of a research line dedicated to the application of MDO strategies to small vertical takeoff and landing (VTOL) vehicles. Apart from being useful for different applications, such vehicles also offer the possibility of experimentally validating design strategies and decisions due to their low cost and easier manufacturing and flight testing (compared to bigger vehicles) procedures. On the other hand, manufacturing the vehicle is usually a time consuming task that includes not only the fabrication itself but also the generation of 3D models, needed to guide the integration of all the systems. Building a good model often requires experience to avoid several iterations and minimize cost. In [22], we developed a simplified MDO problem to design a vehicle for the 2022 International Micro Aerial Vehicle Competition. The outcome of this problem was a set of parameters, shown in Tab.1. In order to "transform" such numbers into a real vehicle, we manually built the 3D model shown in Fig.1. Such process consumed significantly more time than running the MDO. Similarly, in [18] we fabricated propellers to compare different aerodynamic techniques for evaluating their performance. After designing one by defining its airfoils, twist and chord distributions, a manual 3D model was also needed to design the hub and integrate it with the blades in order to have a usable propeller. This papers addresses this gap between the output of a given MDO problem and the generation of a manufacturing compliant 3D model, allowing for time and cost reduction

Table 2: Wing section parameters.

Parameter	Unit
Chord	[m]
Position in X , Y , and Z	[m]
Twist angle	[deg]
Airfoil location of max camber	[percent chord]
Airfoil maximum thickness	[percent chord]
Airfoil maximum camber	[percent chord]

and permitting less experienced designers to build models more easily.

3 DATA SHARING

In the subsequent sections, we outline the methodology utilized and present the results obtained. All files, ESP geometries and Python scripts, are shared so the community can use and improve the methods. They are available in *ENAC drones* group *GitHub* at https://github.com/enac-drones/AeroBest23_MDO_UAV/tree/paper_codes/. We provide two examples for wings manufacturing, one simpler without twist and using a NACA airfoil (under *Wo_twist* folder) and other with twist and Kulfan airfoils (under *With_twist* folder). The scripts using ESP’s Python interface for wing weight estimation are also provided. The Python scripts for blade generation and ESP files for propellers are available under the folder *propellers*.

4 METHODOLOGY

Instead of defining an MDO process, we only represent the output of such kind of problem, ensuring that the same strategy can be used for any process with a similar parametrization. As explained by Hajdik *et al.* [23], despite the wide application of free form deformation (FFD) in MDO, as in [24–26], coupling FFD geometries in general design and manufacturing workflows is not straightforward, as information might be lost throughout this process. So, a CAD tool is employed, specifically the *Engineering Sketch Pad* (ESP) [27], an open source and operating system agnostic software. ESP incorporates drivers for aerodynamic and structural tools. Additionally, it is compatible with OpenM-DAO [28] and natively allows for gradient calculation. In order to test our proposal for wings, we select a representative set of design parameters and present the different modeling strategies needed for manufacturing and for mass/inertia estimation. For propellers, the manufacturing process is simpler and relies on *BladeX* by Gadalla *et al.* [29].

4.1 Wing and propeller parametrization

Each wing section is defined by the parameters shown in Tab.2, where the number of sections can also change. ESP has primitives for different airfoil families, but we employ NACA family for simplicity. The structural parameters, shown in Tab.3, are defined for the whole wing. Spars are assumed to be cylindrical as off-the-shelf carbon tubes are usually employed in this form for small UAVs. The rib offset is the angle between the ribs and the chord line. For propeller parametrization we employ three parameters: airfoil(s), chords and twist distributions along the radius.

Table 3: Wing structural parameters.

Parameter	Unit
Number of ribs	-
Thickness of the ribs	[m]
Ribs offset	[deg]
Number of spars	-
Diameter of each spar	[m]
Location of each spar	[percent chord]

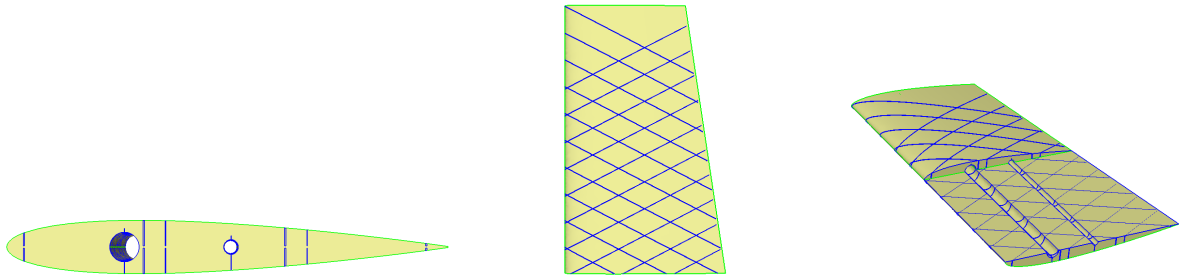


Figure 2: Modeling the wing to comply with the manufacturing technique: solid body with empty internal ribs (in detail on the right) and spars.

4.2 Manufacturing setup

The wings are manufactured with a *Raise3D N2 Pro* by *Raise 3D*¹. We use the lightweight PLA from *colorFabb*² for all tests. Once the geometry has been defined, as an *STL* file for our case, it needs to be "sliced" in order to be printed. There are several open source slicers. We use the *IdeaMaker*³ due to its compatibility with our printers. For the propeller, the 3D printer *Form 3+*, from *FORMLABS*⁴ is employed. The material used is the "Tough" resin, provided by the same company. To prepare the printing process we use the *PreForm*⁵, also open source.

4.3 Modeling wings for manufacturing

The 3D printing process is based on the one presented in [30] and has already been used in [22]. This fabrication strategy ensures a more continuous printing, minimizing the need to remove the nozzle throughout the process, which tends to increase the weight of the piece and reduce its quality. It roughly consists in modeling the wing as a solid body while keeping the ribs as empty cavities. Figure 2 shows the obtained model. *ESP* is capable of directly outputting the resulting geometry as an *STL* file, which is then used to obtain the *G code* needed to print the part. Manufacturing wings with high twist angles and cambered airfoils might require some adaptations to the original method in order to

¹www.raise3d.com

²www.colorfabb.com

³www.ideamaker.io

⁴www.formlabs.com/eu/3d-printers/form-3

⁵www.formlabs.com/eu/software/#preform

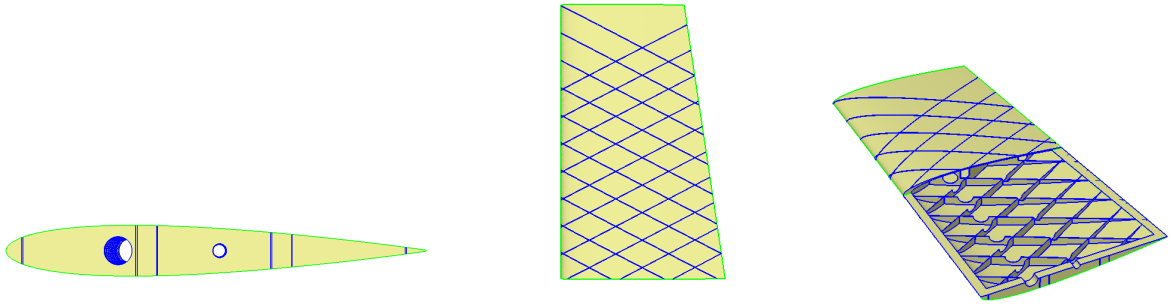


Figure 3: Modeling the real printed wing for mass and inertia estimation, with internal ribs being detailed on the right.

Table 4: *Masstran* material definition.

Parameter	value
Material	Lighweight PLA
Material density	390 [$\frac{kg}{m^3}$]
Material type	Isotropic shell
Membrane thickness	0.74[mm]

correctly generate the ribs. An example for such case is also available for comparison.

4.4 Modeling wings for mass and inertia estimation

Understanding the modelization strategy for mass and inertia estimation is straightforward. The CAD model needs to represent the final manufactured body as accurately as possible, as seen in Fig.3. With such model and the material definition, shown in Tab.4, we calculate mass and inertia with the *Masstran* feature present in *PyCaps* [31]. The membrane thickness was obtained after averaging different printed pieces.

4.5 Modeling propellers

The propeller process starts with the definition of one blade using BladeX [29]. The blade is defined by means of its airfoils and chord and twist distributions. Once the blade is generated, it is exported as an *IGES* file. The ESP script then imports this file to generate both blades. It also models the hub and exports the propeller as an *STL* file to be used for printing.

5 RESULTS

In the following sections we present the results obtained with the manufacturing processes as well as some aspects regarding their validation. We present the comparison between predicted and measured weight for wings and discuss the time needed to obtain the printed pieces.

5.1 Wings

Figure 4 shows two printed wings, different from each other because of the airfoils, geometric twist and number of ribs, and also a zoom in the airfoil and wing internal



(a) Printed wings with and without twist.



(b) Airfoil and internal structure.

Figure 4: Printed wings.



(a) Twisted wing with 3 ribs per side.



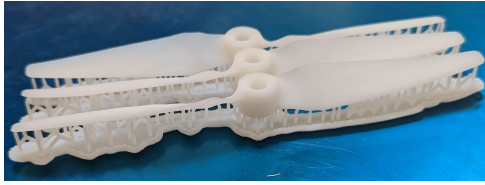
(b) Straight wing with 10 ribs per side.

Figure 5: Wing mass measurements.

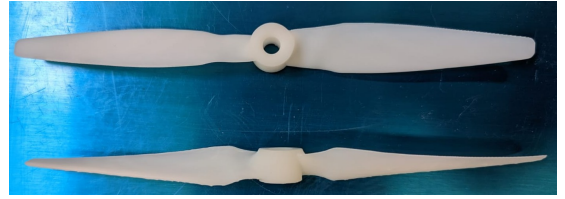
structure. The geometry of the wings can for now be validated by means of measuring span and chord. A further analysis with 3D scanners is left for future work. However, any mismatch between the printed wing and the one defined during the optimization is most likely caused by the printing itself, as the geometry generated with ESP matches the one intended. We also compare the expected and observed mass using *Masstran* from *PyCaps* [31]. Each wing mass was measured and the results are shown in Fig.5. Table 5 shows the difference between predicted and measured mass. The accuracy of the outcome is highly dependent on the quality of the mass models. For more complex wings with, for example, command surfaces, servos, and hinges, the prediction might lose precision, depending on how such geometry is modeled. For our case, the simple wing geometry is

Table 5: Mass prediction results.

Number of ribs	Masstran result [g]	Measured mass [g]	Error [%]
3	25.30	26.1 ± 0.1	3.16
10	31.53	29.5 ± 0.1	6.88



(a) Printed propellers straight out of the printer.



(b) After the cleaning and "sanding" process.

Figure 6: Printed propellers.

based on our vehicle Falcon [22] shown in Fig.1, a UAV with four motors and no command surfaces. As *Masstran* also is capable of calculating inertia, this tool can be very useful for flight dynamics analysis. However, any validation with this regard is left for future work. The CAD model and "manufacturing view" are automatically generated once the geometry is known. So the total time to obtain the piece is driven by the manual slicing process, which is straightforward, and the printing time. The printing time depends highly on the geometry, printer, and material. For both wings manufactured for this paper, the process took roughly 4 hours each considering the setup presented in Section 4.2. This result shows a potential of reducing the manufacturing time in days where the final goal is to have only the printing time as constraint. However, the real reduction is hard to estimate because it highly depends on the designer's ability to generate the model and on the complexity of the geometry.

5.2 Propellers

Figure 6 shows the obtained propellers. The printer generates a supporting structure to ensure quality, as shown in Fig.6a. This structure needs to be removed and the propeller cleaned, as shown in Fig.6b. We can also validate propellers by measuring the chords and twist angles. The 3D scan technology is even more important for them as it is difficult to measure the angles properly. However, the similar performance in experiments and analytical methods observed in [18] indicates that the propellers are close to the original geometry definition.

6 CONCLUSION

In this paper, we present a preliminary way of integrating the manufacturing process of wings and propellers to an MDO framework for UAVs. We employ ESP to automatically generate the fabrication and mass prediction geometric "views". Such geometries are then used to manufacture two sample wings and assess their predicted weight. The weight prediction shows good accuracy for our case, mainly because of the simplicity of the wings analyzed. We also present a similar strategy for propeller manufacturing. Such strategy has also been used in [18] and the performance obtained in wind tunnel tests was close to the one expected. It is expected that this solution can improve MDO processes by providing new manufacturing constraints and anticipating potential issues. It can also reduce the time needed to build test vehicles to perform flight and/or wind tunnel test campaigns, thus accelerating the design process. Every script used for this paper is open source so the community can use the methods to build UAVs and subscale vehicles to improve MDO processes.

ACKNOWLEDGEMENTS

This work is part of the activities of ONERA-ISAE-ENAC joint research group.

REFERENCES

- [1] E. Ausonio, P. Bagnerini, and M. Ghio. Drone swarms in fire suppression activities: A conceptual framework. *Drones*, 5(1), 2021. ISSN 2504-446X. doi:10.3390/drones5010017. URL <https://www.mdpi.com/2504-446X/5/1/17>.
- [2] B. Aydin, E. Selvi, J. Tao, and M. J. Starek. Use of fire-extinguishing balls for a conceptual system of drone-assisted wildfire fighting. *Drones*, 3(1), 2019. ISSN 2504-446X. doi:10.3390/drones3010017. URL <https://www.mdpi.com/2504-446X/3/1/17>.
- [3] M. A. Akhloufi, A. Couturier, and N. A. Castro. Unmanned aerial vehicles for wild-land fires: Sensing, perception, cooperation and assistance. *Drones*, 5(1), 2021. ISSN 2504-446X. doi:10.3390/drones5010015. URL <https://www.mdpi.com/2504-446X/5/1/15>.
- [4] Y. Taddia, C. Corbau, J. Buoninsegni, U. Simeoni, and A. Pellegrinelli. Uav approach for detecting plastic marine debris on the beach: A case study in the po river delta (italy). *Drones*, 5(4), 2021. ISSN 2504-446X. doi:10.3390/drones5040140. URL <https://www.mdpi.com/2504-446X/5/4/140>.
- [5] A. Restás. Drone applications fighting covid-19 pandemic;towards good practices. *Drones*, 6(1), 2022. ISSN 2504-446X. doi:10.3390/drones6010015. URL <https://www.mdpi.com/2504-446X/6/1/15>.
- [6] B. Kwak, J. Shintake, L. Zhang, and D. Floreano. Towards edible drones for rescue missions: design and flight of nutritional wings. In *2022 IEEE/RSJ International Conference on Intelligent Robots and Systems (IROS)*, pages 1802–1809, 2022. doi:10.1109/IROS47612.2022.9981956.
- [7] P.-H. Chung, D.-M. Ma, and J.-K. Shiau. Design, manufacturing, and flight testing of an experimental flying wing uav. *Applied Sciences*, 9(15), 2019. ISSN 2076-3417. doi:10.3390/app9153043. URL <https://www.mdpi.com/2076-3417/9/15/3043>.
- [8] G. Nugroho, A. A. Rafsan Jani, R. R. Trio Sadewo, and M. Satrio. Manufacturing process and flight testing of an unmanned aerial vehicle (uav) with composite material. In *Materials and Technologies in Modern Mechanical Engineering*, volume 842 of *Applied Mechanics and Materials*, pages 311–318. Trans Tech Publications Ltd, 9 2016. doi:10.4028/www.scientific.net/AMM.842.311.
- [9] *Mission-Oriented Additive Manufacturing of Modular Mini-UAVs*, 2020. doi:10.2514/6.2020-0064. URL <https://arc.aiaa.org/doi/abs/10.2514/6.2020-0064>.
- [10] *Design Optimization, Fabrication, and Testing of a 3D Printed Aircraft Structure Using Fused Deposition Modeling*, 2020. doi:10.2514/6.2020-1924. URL <https://arc.aiaa.org/doi/abs/10.2514/6.2020-1924>.

- [11] *The Use of MDO and Advanced Manufacturing to Demonstrate Rapid, Agile Construction of a Mission Optimized UAV*, 2013. doi:10.2514/6.2013-1675. URL <https://arc.aiaa.org/doi/abs/10.2514/6.2013-1675>.
- [12] J. F. Laliberté, K. L. Kraemer, J. W. Dawson, and D. Miyata. Design and manufacturing of biologically inspired micro aerial vehicle wings using rapid prototyping. *International Journal of Micro Air Vehicles*, 5(1):15–38, 2013. doi:10.1260/1756-8293.5.1.15. URL <https://doi.org/10.1260/1756-8293.5.1.15>.
- [13] N. Atlas. World’s first jet-powered, 3d-printed uav debuts at dubai airshow, 2015. URL <https://newatlas.com/worlds-largest-fastest-3d-printed-uav/40293/>.
- [14] G. Goh, S. Agarwala, G. Goh, V. Dikshit, S. Sing, and W. Yeong. Additive manufacturing in unmanned aerial vehicles (uavs): Challenges and potential. *Aerospace Science and Technology*, 63:140–151, 2017. ISSN 1270-9638. doi:<https://doi.org/10.1016/j.ast.2016.12.019>. URL <https://www.sciencedirect.com/science/article/pii/S127096381630503X>.
- [15] *Aero-engine model design and assembly practice teaching based on 3D printing*, 2023. doi:10.2514/6.2023-1020. URL <https://arc.aiaa.org/doi/abs/10.2514/6.2023-1020>.
- [16] I. Rêgo, T. Marcos, D. R. Pinto, R. Vilela, V. Galvão, A. Pivetta, G. Camilo, J. Silva, B. Lima, A. Carvalhal, R. Cardoso, J. Martos, A. Santos, A. Oliveira, and P. Toro. Ground experimentation with 3d printed scramjet inlet models at hypervelocities. *Aerospace Science and Technology*, 55:307–313, 2016. ISSN 1270-9638. doi:<https://doi.org/10.1016/j.ast.2016.06.009>. URL <https://www.sciencedirect.com/science/article/pii/S1270963816302188>.
- [17] B. Rutkay and J. Laliberté. Design and manufacture of propellers for small unmanned aerial vehicles. *Journal of Unmanned Vehicle Systems*, 4(4):228–245, 2016. doi:10.1139/juvs-2014-0019. URL <https://doi.org/10.1139/juvs-2014-0019>.
- [18] L. F. Fernandez, M. Bronz, N. Bartoli, and T. Lefebvre. Assessment of methods for propeller performance calculation at high incidence angles. In *AIAA SCITECH 2023 Forum*, 2023. doi:10.2514/6.2023-2283. URL <https://arc.aiaa.org/doi/abs/10.2514/6.2023-2283>.
- [19] *Bringing Manufacturing into the MDO domain using MBSE*, 2022. doi:10.2514/6.2022-3721. URL <https://arc.aiaa.org/doi/abs/10.2514/6.2022-3721>.
- [20] G. Donelli, P. D. Ciampa, B. Nagel, G. Lemos, J. Mello, A. P. C. Cuco, and T. van der Laan. A model-based approach to trade-space evaluation coupling design-manufacturing-supply chain in the early stages of aircraft development. In *AIAA AVIATION 2021 FORUM*, 2021. doi:10.2514/6.2021-3057. URL <https://arc.aiaa.org/doi/abs/10.2514/6.2021-3057>.

- [21] G. Donelli, P. D. Ciampa, T. Lefebvre, N. Bartoli, J. M. Mello, F. I. Odaguil, and T. van der Laan. Value-driven model-based optimization coupling design-manufacturing-supply chain in the early stages of aircraft development: Strategy and preliminary results. In *AIAA AVIATION 2022 Forum*, 2022. doi:10.2514/6.2022-3723. URL <https://arc.aiaa.org/doi/abs/10.2514/6.2022-3723>.
- [22] L. F. T. Fernandez, M. Bronz, N. Bartoli, and T. Lefebvre. Development of a mission-tailored tail-sitter mav. In *13th International Micro Air Vehicle Conference*, pages 159–168, Delft, the Netherlands, Sep 2022. URL <http://www.imavs.org/papers/2022/19.pdf>. Paper no. IMAV2022-19.
- [23] *Aerodynamic Shape Optimization with CAD-Based Geometric Parameterization*, 2023. doi:10.2514/6.2023-0726. URL <https://arc.aiaa.org/doi/abs/10.2514/6.2023-0726>.
- [24] G. K. W. Kenway, G. J. Kennedy, and J. R. R. A. Martins. A CAD-free approach to high-fidelity aerostructural optimization. In *Proceedings of the 13th AIAA/ISSMO Multidisciplinary Analysis Optimization Conference*, Fort Worth, TX, September 2010. AIAA 2010-9231.
- [25] Y. Shi, C. A. Mader, and J. R. R. A. Martins. Natural laminar flow wing optimization using a discrete adjoint approach. *Structural and Multidisciplinary Optimization*, 64(2):541–562, Aug 2021. ISSN 1615-1488. doi:10.1007/s00158-021-02936-w. URL <https://doi.org/10.1007/s00158-021-02936-w>.
- [26] N. P. Bons, J. R. R. A. Martins, F. I. K. Odaguil, and A. P. C. Cuco. Aerostructural Wing Optimization of a Regional Jet Considering Mission Fuel Burn. *ASME Open Journal of Engineering*, 1, 10 2022. ISSN 2770-3495. doi:10.1115/1.4055630. URL <https://doi.org/10.1115/1.4055630>. 011046.
- [27] J. Dannenhoffer and R. Haimes. The engineering sketch pad, 2022. URL <https://acdl.mit.edu/esp/>.
- [28] J. S. Gray, J. T. Hwang, J. R. R. A. Martins, K. T. Moore, and B. A. Naylor. OpenMDAO: An open-source framework for multidisciplinary design, analysis, and optimization. *Structural and Multidisciplinary Optimization*, 59(4):1075–1104, April 2019. doi:10.1007/s00158-019-02211-z.
- [29] M. Gadalla, M. Tezzele, A. Mola, and G. Rozza. BladeX: Python Blade Morphing. *The Journal of Open Source Software*, 4(34):1203, 2019. doi:<https://doi.org/10.21105/joss.01203>.
- [30] T. Station. How i designed a 3d printed wing. URL https://www.youtube.com/watch?v=QJjhMan6T_E.
- [31] R. J. Durscher and D. Reedy. pycaps: A python interface to the computational aircraft prototype syntheses. In *AIAA Scitech 2019 Forum*, 2019. doi:10.2514/6.2019-2226. URL <https://arc.aiaa.org/doi/abs/10.2514/6.2019-2226>.